Supplementary Information I: Model description

Competition alters predicted forest carbon cycle responses to nitrogen availability and elevated CO_2: simulations using an explicitly competitive, game-theoretic vegetation demographic model

Ensheng Weng[1,2], Ray Dybzinski[3], Caroline E. Farrior[4], Stephen W. Pacala[5]

[1]Center for Climate Systems Research, Columbia University, New York, NY 10025

[2]NASA Goddard Institute for Space Studies, 2880 Broadway, New York, NY 10025

[3]Institute of Environmental Sustainability, Loyola University Chicago, Chicago, IL 60660

[4] Department of Integrative Biology, University of Texas at Austin, Austin, TX 78712

[5]Department of Ecology & Evolutionary Biology, Princeton University, Princeton, NJ 08544

Email: wengensheng@gmail.com

Phone: 212-678-5585

Table of content

Supplementary Information I: BiomeE model description

A. Light harvest, photosynthesis, stomatal conductance and respiration

Light harvest

In BiomeE, same as LM3-PPA, individual trees are represented as sets of *cohorts* of similar size trees and are arranged in different vertical canopy layers according to their height and crown area following the rules of the Perfect Plasticity Approximation (PPA) (Strigul et al., 2008) (Fig. A1). The PPA model allows for flexibility in the shapes of individual tree crowns (Purves et al., 2008; Strigul et al., 2008), but for simplicity, we assume that trees have flat-topped crowns, which allows for accurate predictions of observed succession and canopy structure in broad-leaved temperate forests (Purves et al., 2008) and canopy structure in a Neotropical forest (Bohlman and Pacala, 2012).

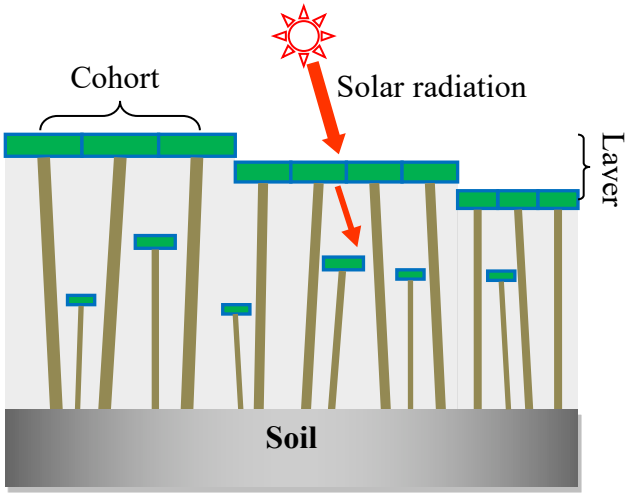

Figure A1 Community structure and light partitioning

Individual tree height is defined as the height at the top of the crown, and all foliage of a given cohort is assumed to belong to a single canopy layer. The height of canopy closure for

layer k (k =1 is the top layer, k = 2 is the second layer, etc.) is referred to as Z_k^*, the height of the shortest tree in the layer, and is defined implicitly by the following equation:

$$k(1-\eta) = \sum_i \int_{Z_k^*}^{\infty} N_i(Z,t) A_{CR,i}(Z_k^*, Z) dZ \qquad \text{(A1)}$$

where $N_i(Z,t)$ is the density of PFT i trees of height Z per unit ground area; $A_{CR,i}(Z_k^*, Z)$ is the crown area of an individual PFT i tree of height Z; and η is the proportion of each canopy layer that remains open on average due to spacing between individual tree crowns.

The top layer includes the tallest cohorts of trees whose collective crown area sums to $1-\eta$ times the ground area, and lower layers are similarly defined. Trees within the same layer do not shade each other, but there is self-shading among the leaves within individual crowns. Cohorts in a sub-canopy layer are shaded by the leaves of all taller canopy layers using a mean field approximation; i.e., in a given canopy layer, all cohorts are assumed to have the same incident radiation on the top of their crowns (Fig. A1). The gap fraction η increases light penetration through each canopy layer and allows for the persistence of understory trees in monoculture forests in which the upper canopy builds a physiologically-optimal number of leaf layers, i.e. one in which its lowest leaves are at zero carbon balance (Farrior et al., 2013).

Photosynthesis and stomatal conductance

We use the photosynthesis model of LM3-PPA to calculate photosynthesis rate and transpiration of vegetation. This model first calculates the net carbon assimilation rate (photosynthesis) and stomatal conductance of the leaves of each tree (cohort), integrated through the leaf area within a cohort's canopy, in the absence of soil water limitation. These values of assimilation and stomatal conductance require a certain water demand. Then, it calculates available water supply, and reduce the demand-based assimilation and stomatal conductance

accordingly if water supply is less than water demand. The water-demand-based photosynthesis and stomatal conductance equations for a well-watered plant are modified from Farquhar et al. (1980), Collatz et al. (1992, 1991), and Leuning et al. (1995). We present equations for both C_3 and C_4 plants, although only the former are included in the examples presented in this paper. The model assumes that the entire canopy of a given cohort is isothermal with temperature T_v, and the air in the intercellular spaces is water-saturated with specific humidity equal to saturated specific humidity $q^*(T_v)$. The link between stomatal conductance (g_s, mol m^{-2} s^{-1}), the rate of net photosynthesis (A_n, mol CO_2 m^{-2} s^{-1}), intercellular concentration of CO_2 (C_i, mol CO_2 mol^{-1} air), and the difference in specific humidity between the intercellular spaces and the canopy air (q_a, kg H_2O kg^{-1}air) can be expressed as a simplification of Leuning's (1995) empirical relationship assuming negligible cuticular conductance:

$$g_s = \frac{mA_n}{(C_i - \Gamma_*)\cdot(1+(q^*(T_v)-q_c)/d_0)} \quad \text{(A2)}$$

where m is the slope of the stomatal conductance relationship, d_0 is a reference value of canopy air water vapor deficit (kg H_2O kg^{-1} air), and Γ^* (mol CO_2 mol^{-1} air) is the CO_2 compensation point:

$$\Gamma^* = \alpha_c[O_2]\frac{K_C}{K_O} \quad \text{(A3)}$$

where $\alpha_c = 0.21$ is the maximum ratio of oxygenation to carboxylation, $[O_2]$ is the concentration of oxygen in canopy air (0.209 mol O_2 mol^{-1} air), and K_C (mol CO_2 mol^{-1} air) and K_O (mol O_2 mol^{-1} air) are the Michaelis-Menten constants for CO_2 and O_2, respectively. K_C and K_O depend on temperature according to an Arrhenius function:

$$f_A(E_0,T) = e^{E_0\left(\frac{1}{298.15}-\frac{1}{T}\right)} \quad \text{(A4)}$$

where $K_C = D_C f_A(E_{0,C}, T_v)$ and $K_O = D_O f_A(E_{0,O}, T_v)$, with respective constants: $D_C = 1.5\times10^{-4}$ mol CO_2 mol^{-1} air , $E_{0,C} = 6000$ K, $D_O = 0.25$ mol O_2 mol^{-1} air, and $E_{0,O} = 1400$ K.

Net photosynthesis A_n can be expressed as a CO_2 diffusive flux between canopy air and the stomata (Leuning et al., 1995):

$$A_n = \frac{g_s}{1.6} \cdot (C_a - C_i) \tag{A5}$$

where C_a is the concentration of CO_2 in the canopy air, and the factor 1.6 is the ratio of diffusivities for water vapor and CO_2. We assume that the diffusion of CO_2 is mostly limited by stomatal conductance and not by the leaf boundary layer conductance, which we ignore for simplicity, following the formulation of the ED model (Medvigy et al., 2009; Moorcroft et al., 2001). Combining Eqs. A2 and A5 yields the intercellular concentration of CO_2:

$$C_i = \frac{C_a + \Gamma_* \frac{1.6}{m}\left(1 + \frac{q^*(T_v) - q_a}{d_0}\right)}{1 + \frac{1.6}{m}\left(1 + \frac{q^*(T_v) - q_a}{d_0}\right)}. \tag{A6}$$

Following the mechanistic photosynthesis model of Farquhar et al.(1980), with extensions introduced by Collatz et al. (1992, 1991), we can also express net photosynthesis (A_n) as the difference between gross photosynthesis and leaf respiration, and assume gross photosynthesis is the minimum of several physiological process rates:

$$A_n = f_T(T_v)\left[\min\left(J_E, J_C, J_j\right) - \gamma V_m(T_v)\right] \tag{A7}$$

where $f_T(T_v)$ is a thermal inhibition factor (see below); J_E, J_C, and J_j are light limited, Rubisco (CO_2) limited, and export limited rates of carboxylation, respectively; $V_m(T_v)$ is the maximum carboxylation velocity (mol CO_2 m^{-2} s^{-1}); and γ is a constant relating leaf respiration to V_m. The thermal inhibition factor, assumed to affect carbon acquisition and respiration equally, is

$$f_T(T_v) = \frac{1}{[1+\exp(0.4(5^\circ\mathrm{C} - T_v))][1+\exp(0.4(T_v - 45^\circ\mathrm{C}))]}. \quad \text{(A8)}$$

99 The maximum carboxylation velocity, V_m, depends on the temperature of the leaf:

$$V_m(T_v) = V_{\max} f_A(E_V, T_v) \quad \text{(A9)}$$

100 where V_{max} (the reference value of V_m, at 25° C) is a species-specific constant, $f_A(T_v)$ is given by

101 Eq. B3.3, and E_v is the activation energy (see Appendix C).

102 For C_3 plants, Collatz et al. (1991):

$$J_E = a\alpha_{LUE} Q \frac{C_i - \Gamma_*}{C_i + 2\Gamma_*} \quad \text{(A10 a)}$$

$$J_C = \frac{V_m(T_v)(C_i - \Gamma_*)}{C_i + K_c(T_l)\frac{p_{ref}}{p} \cdot \left(1 + \frac{p}{p_{ref}} \frac{[O_2]}{K_o(T_l)}\right)} \quad \text{(A10 b)}$$

$$J_j = \frac{V_m(T_v)}{2} \quad \text{(A10 c)}$$

103 where a is the leaf absorptance of photosynthetically-active radiation (PAR), Q is incident PAR

104 per unit leaf area (E m^{-2} s^{-1}), α_{LUE} is the intrinsic quantum efficiency of photosynthesis (mol CO_2

105 E^{-1}), p is atmospheric pressure, and P_{ref} is the reference atmospheric pressure (1.01×10^5 Pa).

106 For C_4 plants, A_n is calculated by a similar equation as Eq. A7 according to Collatz et al.

107 (1992) . The rate of carboxylation is calculated by the minimum of the rates limited by light,

108 maximum carboxylation velocity, and CO_2 as shown in the following:

$$J_E = a\alpha_{LUE} Q \quad \text{(A11 a)}$$

$$J_C = V_m(T_v) \quad \text{(A11 b)}$$

$$J_{CO2} = 18000 V_m(T_v) C_i \qquad \text{(A11 c)}$$

The solution of the Eqs A7~A11 yields net (A_n) and gross photosynthesis rates for a thin canopy layer with incident PAR flux Q per unit leaf area. We now solve for the photosynthesis integrated through the depth of a cohort's canopy, given incident PAR flux Q calculated according to the two-stream approximation described in Weng et al. (2015). Q is assumed to decrease exponentially, according to Beer's law, through the depth of a cohort's canopy: $Q(l) = Q_0 \exp(-\kappa l)$, where Q_0 is incident PAR at the top of the cohort's canopy, and l is the overlying leaf area per crown area at a given depth within the cohort's canopy, with $L = 0$ at the top of the cohort's crown, and $l = LAI$ at the bottom (here, "LAI" is the total leaf area per crown area of a cohort's canopy). The Beer's law extinction coefficient κ is calculated as a function of the zenith angle of solar radiation (which varies by latitude, time of day, and day of year) and leaf angle distribution in the canopy (assumed spherical) to approximate the attenuation of photosynthetically-active radiation within a single cohort's canopy according to the two-stream approximation. We can define a depth l_{eq} where the light-limited rate J_E is equal to the minimum of other limiting rates. Gross photosynthesis below depth l_{eq} (the integral in Eq. A12 below) is a function of light availability, while above this depth it is equal to the minimum of other limiting rates. The net photosynthesis averaged over the entire canopy depth can be expressed as

$$\overline{A}_n = \frac{f_T(T_v)}{LAI}\left[J_{\min} l_{eq} + \int_{l_{eq}}^{LAI} J_E(l)\,dl \right] - f_T(T_v)\gamma V_m(T_v) \qquad \text{(A12)}$$

where

$$J_{\min} = \begin{cases} \min(J_C, J_j) & \text{for C}_3 \text{ plants} \\ \min(J_C, J_{CO2}) & \text{for C}_4 \text{ plants} \end{cases}$$

If incident light Q_0 is so low that no part of canopy is light-saturated, then $l_{eq} = 0$.

Using the Beer's law approximation of the light profile within a cohort's canopy, we can obtain the following expressions for the integral in Eq. A12:

$$\int_{l_{eq}}^{LAI} J_E(l)dl = a\alpha' Q_0 \frac{\exp(-kl_{eq}) - \exp(-kl)}{k} \quad \text{(A13)}$$

and for l_{eq}:

$$l_{eq} = \frac{1}{k}\log\left(\frac{a\alpha' Q_0}{J_{\min}}\right) \quad \text{(A14)}$$

where, $\alpha' = \alpha \frac{C_i - \Gamma_*}{C_i + 2\Gamma_*}$ for C_3 plants and $\alpha' = \alpha$ for C_4 plants.

Average stomatal conductance is calculated from Eqs. A2 and A12:

$$\overline{g_s} = \max\left(\frac{m\overline{A_n}}{(C_i - \Gamma_*)\cdot(1 + (q^*(T_v) - q_a)/d_0}, g_{s,\min}\right) \quad \text{(A15)}$$

where $g_{s,min}$ = 0.01 mol H_2O m^{-2} s^{-1} is the minimum stomatal conductance allowed in the model.

The model applies some further corrections to the net photosynthesis and stomatal conductance calculations above for a well-watered plant, in order to take into account limitations imposed by water availability and other factors:

$$\overline{\overline{A_n}} = \phi_w \phi_i \phi_m \overline{A_n} \quad \text{(A16)}$$

$$\overline{\overline{g_s}} = \phi_w \phi_i \phi_m \overline{g_s} \quad \text{(A17)}$$

where ϕ_w is the reduction due to water limitations, ϕ_i is reduction due to presence of intercepted water and snow on leaves, and ϕ_m is the imposed maximum conductance limitation. If there is water or snow on the canopy, the photosynthesis is reduced proportionally to the covered fraction of leaves:

$$\phi_i = 1 - (f_l + f_s)\alpha_{wet} \quad \text{(A18)}$$

where f_l and f_s are the fractions of canopy covered by liquid water and snow, respectively; α_{wet} is the down-regulation coefficient, assumed to be 0.3; i.e., photosynthesis of leaves fully covered by water or snow is reduced by 30% compared to dry leaves.

The model also imposes an upper limit on stomatal conductance. If the calculated $\overline{g_s}$ is higher than the limit $g_s^{\max} = 0.25$ mol m^{-2} s^{-1}, then stomatal conductance and net photosynthesis are adjusted:

$$\phi_m = \begin{cases} g_s^{\max} / \overline{g_s}, & \overline{A_n} > 0 \\ 1, & \overline{A_n} \le 0 \end{cases} \quad \text{(A19)}$$

Finally, stomatal conductance and photosynthesis are adjusted down if available water demand is greater than water supply. Given mean stomatal conductance $\overline{g_s}$ (Eq. A15), the water demand per individual (kg/s) is:

$$U_d = \overline{\overline{g_s}} M_{air} (q^*(T_v) - q_a) A_{leaf} \quad \text{(A20)}$$

where M_{air} is the mass of air per mol (g mol^{-1}), used to convert stomatal conductance to mass units, and A_{leaf} is the total area of leaves in the individual's canopy.

Given the water supply (i.e., the maximum plant water uptake rate, $U_{\max}$), which is defined as the uptake rate when root water potential is at the plant permanent wilting point, net photosynthesis and stomatal conductance are adjusted for water limitation according to Eqs. A16 and A17 using the factor:

$$\phi_w = \min(U_{\max} / U_d, 1). \quad \text{(A21)}$$

See section F for the details of root water uptake and soil water dynamics.

Autotrophic respiration

The total autotrophic respiration rate of an individual is the sum of maintenance respiration of living tissues and the growth respiration for building new tissues.

$$R_a = R_L + R_{SW} + R_{FR} + r_g(G_W + G_L + G_{FR} + G_F) \quad \text{(A22)}$$

where R_L, R_{SW}, and R_{FR} are the maintenance respirations of leaves, sapwood, and fine roots, and r_g is a growth respiration constant (r_g = 0.33 g C g^{-1} C). Maintenance respiration terms are calculated as:

$$R_L = \gamma_{Leaf} V_{max} A_L \varepsilon \quad \text{(A23.1)}$$

$$R_{SW} = \beta_{SW} A_{CB} f_T \varepsilon' \quad \text{(A23.2)}$$

$$R_{FR} = \beta_{FR} FR f_T \varepsilon' \quad \text{(A23.3)}$$

where γ_{Leaf}, is a respiration coefficient of leaves; ε is a factor converting the unit of carboxylation rate V_{cmax} (mol m^{-2} s^{-1}) to kg C m^{-2} yr^{-1}; β_{SW}, and β_{FR} are respiration coefficients of sapwood and fine roots, respectively (kg C m^{-2} yr^{-1} for sapwood and kg C kg^{-1} C yr^{-1} for fine roots); ε' is a factor converting the unit of kg C m^{-2} yr^{-1} to kg C m^{-2} day^{-1}); A_{CB} is cambium surface area (m^2), which we assume scales with diameter with an exponent 1.5 ($A_{CB} \propto D^{1.5}$), consistent with the height allometry exponent θ_Z = 0.5; and f_T is a temperature-dependent function adapted from Collatz et al. (1991; 1992) that scales respiration rate with temperature:

$$f_T = \frac{\exp\left[3000\left(\frac{1}{288.16} - \frac{1}{T+273.16}\right)\right]}{\{1+\exp[0.4(5-T)]\}\{1+\exp[0.4(T-45.0)]\}} \quad \text{(A24)}$$

where T is ˚C.

B. Nitrogen uptake

The rate of nitrogen uptake (U, g N m^{-2} hour^{-1}) from the soil mineral nitrogen pool is an asymptotically increasing function of fine root biomass density ($C_{\mathrm{FR,total}}$, kgC m^{-2}), following McMurtrie *et al*. (2012)

$$U = f_{\mathrm{U,max}} \cdot N_{\mathrm{mineral}} \cdot \frac{C_{\mathrm{FR,total}}}{C_{\mathrm{FR,total}} + K_{FR}}, \quad \text{(B1)}$$

where, N_{mineral} is the mineral N in soil (g N m^{-2}), $f_{\mathrm{U,max}}$ is the maximum rate of nitrogen absorption per hour when $C_{\mathrm{FR,total}}$ approaches infinity, K_{FR} is a shape parameter (kg C m^{-2}) at which the nitrogen uptake rate is half of the parameter f_{U},max. The nitrogen uptake rate of an individual tree (U_{tree}, g N hour^{-1} tree^{-1}) is calculated as follows:

$$U_{\mathrm{tree}} = U \cdot \frac{C_{\mathrm{FR,tree}}}{C_{\mathrm{FR,total}}}, \quad \text{(B2)}$$

where, $C_{\mathrm{FR,tree}}$ is the fine root biomass of a tree (kgC tree^{-1}). The nitrogen absorbed by roots enters into the NSN pool and then is allocated to plant tissues through plant growth.

For limiting N uptake in an N-rich soil, we define a target NSN (NSN*), which is a function of leaf's target biomass, C:N ratio, and lifespan and root's target biomass and C:N ratio:

$$NSN^{*} = q_N \cdot \left(\frac{L^{*}(D)}{\lambda \cdot CN_{\mathrm{leaf}}} + \frac{FR^{*}(D)}{CN_{FR}}\right), \quad \text{(B3)}$$

where, q_{N} is a constant; λ is leaf lifespan; $L^{*}(D)$ and $FR^{*}(D)$ are the target leaf and fine root biomass at diameter D, respectively; CN_{leaf} and CN_{FR} are the C:N ratios of leaves and fine roots, respectively. $L^{*}(D)$ and $FR^{*}(D)$ are defined in Weng *et al*. (2015). If NSN exceeds the target, then the excess NSN is returned to the mineralized N pool in the soil (i.e. as if it was never taken up to begin with because the plant did not need it).

C. Plant growth and carbon allocation

Allometry

In this model, the partitioning of carbon and nitrogen among these pools are limited by a set of allometric equations and different C:N ratios of these pools. Empirical allometric equations relate woody biomass (including coarse roots, bole, and branches), crown area, and stem diameter. Each individual is composed of six tissues: leaf, fine root, sapwood, heartwood, fecundity, and labile carbon stores (nonstructural carbohydrates, NSC). The individual-level dimensions of a tree, i.e., height (Z), biomass (S), and crown area (A_{CR}) are given by empirical allometries (Farrior et al., 2013):

$$Z(D) = \alpha_Z D^{\theta_Z}$$
$$S(D) = 0.25\pi\Lambda\rho_W\alpha_Z D^{2+\theta_Z} \quad \text{(C1)}$$
$$A_{CR}(D) = \alpha_c D^{\theta_c}$$

where Z is tree height, S is total woody biomass carbon (including bole, coarse roots, and branches) of a tree, α_c and α_Z are PFT-specific constants, θ_c=1.5 and θ_Z=0.5 (Farrior et al. 2013; although they could be made PFT-specific if necessary), π is the circular constant (≈3.1415926), Λ is a PFT-specific constant, and ρ_W is PFT-specific wood density (kg C m^{-3}) .

Following the pipe model (Shinozaki, Kichiro et al., 1964), the *targets* of leaf, fine root, and sapwood cross-sectional area are related by the following equations:

$$L_k^*(D,p) = l_k^* \cdot A_{CR}(D) \cdot \sigma \cdot p(t)$$
$$FR_k^*(D) = \varphi_{RL} \cdot l_k^* \cdot \frac{A_{CR}(D)}{\gamma} \quad \text{(C2)}$$
$$A_{SW,k}^*(D) = \alpha_{CSA} \cdot l_k^* \cdot A_{CR}(D)$$

where L_k^* (D, p) is the target leaf mass of canopy-level k at given stem diameter (D), l_k^* is the target leaf area per unit crown area of a given PFT at canopy-level k, A_{CR}(D) is the crown area of

a tree with diameter D, σ is leaf mass per unit area (LMA), p(t) is a PFT-specific function ranging from zero to one that governs leaf phenology. The phenology function p(t) takes values 0 (non-growing season) and 1 (growing season) (Milly et al., 2014; Shevliakova et al., 2009). The onset of a growing season is controlled by two variables, growing degree days (*GDD*), and a weighted mean daily temperature (T_{pheno}), while the end of a growing season is controlled by T_{pheno}. FR_k^*(D) is the target fine root biomass at diameter D and canopy-level k, φ_{RL} is the ratio of total root surface area to the total leaf area, γ is specific root area, $A^*_{SW,k}(D)$ is the target cross sectional area of sapwood at canopy-level k, and α_{CSA} is an empirical constant (the ratio of sapwood cross-sectional area to target leaf area). All plant tissues are assumed to be 50% carbon by mass.

Plant Growth

Plant growth is co-limited by the availability of carbon and nitrogen. Photosynthate and re-translocated carbon enter the non-structural carbohydrate (NSC) pool, and carbon for respiration, growth, and reproduction are removed from it.

$$\frac{d\,NSC}{dt} = P_s(t) + S_C(t) - R_a(t) - G_C(t), \qquad \text{(C3)}$$

where $G_C(t)$ is the amount of carbon available for producing new plant tissues, including leaves, fine roots, stems, and seeds; S(t) is the carbon retranslocated from senescing leaves and fine roots; $Ra(t)$ is the carbon used for autotrophic respiration; $Ps(t)$ is carbon input from photosynthesis. The carbon fluxes from photosynthesis provide daily total carbon gain from photosynthesis (P_s(t)) and loss from respiration (R_a(t)) for each cohort.

The N absorbed by roots enters the non-structural N (NSN) pool first and then is allocated to the remaining plant pools through plant growth.

$$\frac{dNSN}{dt} = U_N(t) + S_N(t) - G_N(t), \quad \text{(C4)}$$

where, $G_N(t)$ is the amount of nitrogen available for producing new plant tissues from the NSN pool, $S_N(t)$ is the N retranslocated back to NSN from dead leaves and fine roots, $U_N(t)$ is the nitrogen absorbed by roots.

Carbon and nitrogen fetching from their non-structural pools

The available carbon from NSC at time t, $G_C(t)$, is calculated as two components: demand by plant tissues ($G_{C,D}$) and growth tendency driven by NSC ($G_{C,P}$)

$$G_C(t) = Min\begin{pmatrix} G_{C,D} + G_{C,P}, \\ f_{max,C} NSC \end{pmatrix} \quad \text{(C5)}$$

The computations of $G_{C,D}$ and $G_{C,P}$ are based on the "target" amount of leaf mass, $L^*(D, p)$, fine root mass, $FR^*(D)$ and nonstructural carbohydrate, NSC for each cohort. These quantities change with the trunk diameter (D) and its phenological state (p).

We assume plants keep their leaves and fine roots tracking their targets if they have enough carbon in NSC:

$$G_{C,D} = p(t) \cdot [L_k^*(D) + FR_k^*(D) - L_k(t) - FR_k(t)], \quad \text{(C6)}$$

where the subscript k denotes the canopy layer (below, we use the values k=C and k=U for canopy and understory layers, respectively, but this can be generalized to an arbitrary number of layers, k). This component drives leaf flush. The parameter $f_{max,C}$ also defines the rate of leaf flush at the beginning of a growing season (Polgar and Primack, 2011; Wesołowski and Rowiński, 2006). The NSC driven growth during a growing season is defined as:

$$G_{C,P} = p(t) \cdot f_{NSC} \cdot NSC(t), \quad \text{(C7)}$$

where, the parameter f_{NSC} sets the rate of NSC turning to plant tissues (mainly stems).

The nitrogen available for tissue building is:

$$G_N(t) = Min\begin{pmatrix} f_{NSN} \cdot NSN(t) + (L_k^* - L_k(t))/CN_L + (FR_k^* - FR_k(t))/CN_{FR}, \\ f_{max,N} NSN \end{pmatrix}, \quad \text{(C8)}$$

where, f_{NSN} is the rate of NSN turning to plant tissues. The parameters define the strategy of plant growth. If they are great, the plants tend to have a low NSN and NSC pools and grow fast, but are susceptible to bad environment conditions. If they are small, they grow slowly but are safe in bad years because of the high NSN and NSC storage.

Allocation

The carbon and nitrogen allocation rules track PFT-specific targets for leaf area per unit crown area (l^*), fine root area per unit leaf area, a fixed fraction of NPP for reproduction, and the NSC pool size.

Leaves and fine roots have fixed C:N ratios, and so the N removed from NSN to construct new leaves is simply the carbon allocated from NSC to leaves, as calculated in Weng *et al*. (2015), divided by leaf C:N. In cases where there is insufficient NSN to meet the carbon demand for new leaves and roots, the excess carbon is allocated to produce new sapwood. We numerically solve the following equations for the allocation of carbon and nitrogen:

$$G_C \geq G_W + G_L + G_{FR} + G_F \quad \text{(C9.1)}$$

$$G_N \geq \frac{G_L}{CN_{L,0}} + \frac{G_{FR}}{CN_{FR,0}} + \frac{G_F}{CN_{F,0}} + \frac{G_W}{CN_{W,0}} \quad \text{(C9.2)}$$

$$\frac{(FR+G_{FR})\gamma}{(L+G_L)/\sigma} = \varphi_{RL} \quad \text{(C9.3)}$$

$$G_L + G_{FR} = Min\begin{pmatrix} L^* + FR^* - L - FR, \\ f_{LFR,max}\, G_C \end{pmatrix} \cdot r_{S/D} \quad \text{(C9.4)}$$

$$G_F = \left[G_C - Min\begin{pmatrix} L^* + FR^* - L - FR, \\ f_{LFR,max}\, G_C \end{pmatrix} r_{S/D}\right] \cdot v \cdot r_{S/D}\ , \qquad \text{(C9.5)}$$

$$G_W = \left[G_C - Min\begin{pmatrix} L^* + FR^* - L - FR, \\ f_{LFR,max}\, G_C \end{pmatrix} r_{S/D}\right] \cdot \left(1 - v \cdot r_{\frac{S}{D}}\right), \qquad \text{C9.6)}$$

where, $CN_{L,0}$, $CN_{FR,0}$, $CN_{F,0}$, and $CN_{W,0}$ are the target C:N ratios of leaves, fine roots, seeds, and sapwood, respectively; γ is specific root area (m^2 kgC^{-1}); σ is leaf mass per unit area (kgC m^{-2}); $f_{LFR,max}$ is the maximum fraction of G_C for leaves and fine roots (0.85 as default value); v is the fraction of left carbon for seeds (0.1); $r_{S/D}$ is a nitrogen-limiting factor ranging from 0 (no nitrogen for leaves, fine roots, and seeds) to 1 (nitrogen available for full growth of leaves, fine roots, and seeds).

The parameter $r_{S/D}$ controls the allocation of G_C and G_N to the four plant pools. When there is no nitrogen limitation, $r_{S/D}$ equals to 1 and the allocation follows the rules of the carbon only model. In this case, we can solve the potential growth of leaves, fine roots, seed, and stems as:

$$G_L^{'} = \frac{\gamma\sigma\left[FR + Min\begin{pmatrix} L^*+FR^*-L-FR, \\ f_{LFR,max}\, G_C \end{pmatrix}\right] - \varphi_{RL} L}{\gamma\sigma + \varphi_{RL}} \qquad \text{(C10.1)}$$

$$G_{FR}^{'} = \frac{\varphi_{RL}\left[L + Min\begin{pmatrix} L^*+FR^*-L-FR, \\ f_{LFR,max}\, G_C \end{pmatrix}\right] - \gamma\sigma L}{\gamma\sigma + \varphi_{RL}} \qquad \text{(C10.2)}$$

$$G_F^{'} = v\left[G_C - Min\begin{pmatrix} L^* + FR^* - L - FR, \\ f_{LFR,max}\, G_C \end{pmatrix}\right] \qquad \text{(C10.3)}$$

$$G_W^{'} = (1 - v)\left[G_C - Min\begin{pmatrix} L^* + FR^* - L - FR, \\ f_{LFR,max}\, G_C \end{pmatrix}\right] \qquad \text{(C10.4)}$$

Thus, we have the potential nitrogen demand when there is no nitrogen limitation (N'):

$$N' = \frac{G_L'}{CN_{L,0}} + \frac{G_{FR}'}{CN_{FR,0}} + \frac{G_F'}{CN_{F,0}} + \frac{G_W'}{CN_{W,0}}. \quad \text{(C11)}$$

With the solution of nitrogen demand (N'), the analytical solution of can be expressed as:

$$r_{S/D} = Min\left[1, Max\left(0, \frac{G_N - G_C/CN_{W,0}}{N' - G_C/CN_{W,0}}\right)\right], \quad \text{(C12)}$$

where, N'is the potential N demand for plant growth at $r_{S/D}$=1 (i.e., no nitrogen limitation). When $G_N > N'$, all the G_C will be used for plant growth and the excessive nitrogen ($G_N - N'$) will be returned to the NSN pool. When $G_N < G_C/CN_{W,0}$, $r_{S/D}$ equals to 0 and all the G_N will be allocated to sapwood and the excessive carbon ($G_C - G_N CN_{W,0}$) will be returned to NSC pool. This is a very rare case since a low G_N leads to low leaf growth, reducing G_C before the case $G_N < G_C/CN_{W,0}$ happens. Therefore, in most cases, Eq. C9.1 is: $G_C = G_W + G_L + G_{FR} + G_F$.

Tree structure update

The diameter growth and sizes of individual trees are calculated from individual-level allometry and allocation of assimilated carbon. To scale up to a cohort from individual trees, individual pools and fluxes are multiplied by the spatial density of individuals in a cohort. By differentiating the stem biomass allometry in Eq. C1 with respect to time, using the fact that dS/dt equals new sapwood biomass, and rearranging, we have:

$$\frac{dD}{dt} = \frac{G_W}{0.25\pi\Lambda\rho_W\alpha_Z(2+\theta_Z)D^{1+\theta_Z}}. \quad \text{(C13)}$$

The numerator tends to be proportional to $D^{1.5}$ because carbon gain is proportional to crown area, NSC surpluses tend to be a fraction of carbon gain, and crown area is usually roughly proportional to $D^{1.5}$ (Zhang et al., 2014). The denominator tends to be proportional to $D^{1.5}$ because θ_Z tends to be about 0.5 (Zhang et al., 2014). The approximate diameter-independence of

298 Eq C13 allows many aspects of the behavior of the BiomeE model to be understood by referring
299 to analytically tractable versions of the PPA model where *dD*/*dt* is assumed to be independent of
300 *D*.

301 Equations for tree height and crown area growth rates are obtained by differentiating the
302 allometries for Z and A_{CR} in Eq C1 using the chain rule:

$$\frac{dZ}{dt} = \theta_z \alpha_z D^{\theta_z - 1} \frac{dD}{dt} \quad \text{(C14)}$$

$$\frac{dA_{CR}}{dt} = \theta_c \alpha_C D^{\theta_C - 1} \frac{dD}{dt} \quad \text{(C15)}$$

303 The dynamics of leaf biomass of an individual is:

$$\frac{dL}{dt} = G_L p(t) - (1 - p(t)) \cdot \gamma_L L(t) \quad \text{(C16)}$$

304 where γ_L is the PFT-specific rate of leaf senescence triggered by the ending of a growing season.
305 The new leaf biomass is converted into the change in leaf area by dividing by LMA (σ).
306 Similarly, fine root biomass is governed by:

$$\frac{dFR}{dt} = G_{FR}(t) - \gamma_{FR} FR(t). \quad \text{(C17)}$$

307 The total leaf area of a tree is converted to the tree's crown LAI, l_k, by dividing by crown area.

$$l_k = \frac{L_k / LMA}{A_{CR}} \quad \text{(C18)}$$

308

309 **Conversion from sapwood to heartwood**

310 As trees grow, sapwood (SW) is transformed to heartwood (HW). This unidirectional process
311 does not affect the size of the woody biomass C pool. We assume that if the actual sapwood
312 cross-sectional area A_{SW} is larger than its target value, $A^*_{SW}(D)$, the excess portion of sapwood
313 biomass is converted to heartwood. Thus, to determine the amount of sapwood converted to

heartwood in a given time step (*dHW*), we simply calculate the difference between *SW* and the target sapwood C (SW^*) needed to balance L^* and FR^*:

$$dHW = \max(0, SW - SW^*) \quad \text{(C19)}$$

Using the equation for total tree biomass (main text Eq. 4), the target biomass of sapwood is:

$$SW^* = 0.25\pi\Lambda\rho_W\alpha_Z(D^{2+\theta_Z} - {D_{HW}}^{2+\theta_Z}) \quad \text{(C20)}$$

where D is the diameter of the trunk and D_{HW} is the heartwood diameter, which is given by:

$$D_{HW} = 2\sqrt{A_{HW}/\pi} \quad \text{(C21)}$$

where A_{HW} is the cross-sectional area of heartwood. Assuming A_{SW} is at its target value,

$$A_{HW} = A_t - A^*_{SW} \quad \text{(C22)}$$

The cross-sectional area of a trunk (A_t) is:

$$A_t = \pi\left(\frac{D}{2}\right)^2 \quad \text{(C23)}$$

And, according to Eq A2.1 and Eq A2.3, the target cross sectional area of sapwood is defined as:

$$A^*_{SW} = \alpha_{CSA}l^*A_{CR}(D) = \alpha_{CSA}l^*\alpha_C D^{\theta_C} \quad \text{(C24)}$$

D. Population dynamics

Same as the LM3-PPA model (Weng et al. 2015), the BiomeE model predicts population dynamics by simply simulating the birth, mortality, and growth of each cohort. Firstly, the cumulative biomass of seeds produced by a canopy cohort over a growing season of length *T* is converted to seedlings by dividing by the initial plant biomass (S_0) and multiplying by germination and establishment probabilities (p_g and p_e, respectively):

$$N(S_0, t) = \frac{p_g p_e}{S_0} \int_0^T N(\tau) G_F(\tau) d\tau \quad \text{(D1)}$$

where $N(S_0, t)$ is the spatial density of newly generated seedlings, and $N(\tau)$ is the spatial density of the parent cohort at time τ.

After being born, the individuals grow and expand their occupied spaces with resources obtained from leaves (photosynthesis) and roots (water and nitrogen uptake). Let $G_i(s,t)$ denote the multi-dimensional growths of individuals of species i and size s at time t as described in Eqs. C9~C18, then we have:

$$\frac{ds(t)}{dt} = G_i(s, t) \quad \text{(D2)}$$

During growth, the cohorts with organize into canopy layers according to their height and crown area following the rules of PPA (Eq. A1).

The density of individuals in each cohort also decreases as results of mortality due to many reasons (e.g., shading, starvation, disturbances, drought, etc.). Let's assume an overall rate of $\mu(s,t)$:

$$\frac{dN(s,t)}{dt} = -\mu(s, t) N(s, t). \quad \text{(D3)}$$

In BiomeE, mortality is assumed to occur due to carbon starvation if a cohort's NSC pool is close to zero. Because the target size of the NSC pool is assumed to be several times the size of the combined target leaf and fine-root masses, trees rarely die of carbon starvation unless they experience prolonged drought (which was not simulated in the current study) or have chronic negative carbon balance due to shading. In addition to carbon starvation, each species/PFT has a canopy-layer-specific background mortality rate that is assigned from the literature. These background rates are assumed to be size-independent for upper-canopy trees, but size-dependent for understory trees according to:

$$\mu_U(D) = \mu_0 \frac{1+ae^{-bD}}{1+e^{-bD}} \quad \text{(D4)}$$

where, μ0 is species-specific background mortality rate; parameters a and b define the mortality rate changes with tree diameter D. We let *a*=9 and *b*=60 in this study. This functional form reduces mortality by a factor of 5 between germination and adulthood. It accounts for the additional sources of non-starvation mortality facing small individuals, such as herbivory by large mammals and branch-fall.

E. Soil organic matter decomposition and nitrogen mineralization

Each tree consists of seven pools: leaves, fine roots, sapwood, heartwood, fecundity (seeds), and non-structural carbohydrates and nitrogen (NSC and NSN, respectively) (Fig. E1). The carbon and nitrogen in plant pools enter the soil pools with the mortality of individual trees and the turnover of leaves and fine roots. There are three soil organic matter (SOM) pools for carbon and nitrogen: fast-turnover, slow-turnover, and microbial pools, along with a mineral nitrogen pool for mineralized nitrogen in soil. The simulation of SOM decomposition and nitrogen mineralization is based on the models of Gerber *et al*. (2010) and Manzoni *et al*. (2010) and described in detail in Weng et al. (2017). The decomposition rate of a SOM pool is determined by the basal turnover rate together with soil temperature and moisture. The nitrogen mineralization rate is a function of decomposition rate and the C:N ratio of the SOM. Microbes must consume more carbon in the high C:N ratio SOM pool to get enough nitrogen and must release excessive nitrogen in the low C:N ratio SOM pool to get enough carbon for energy.

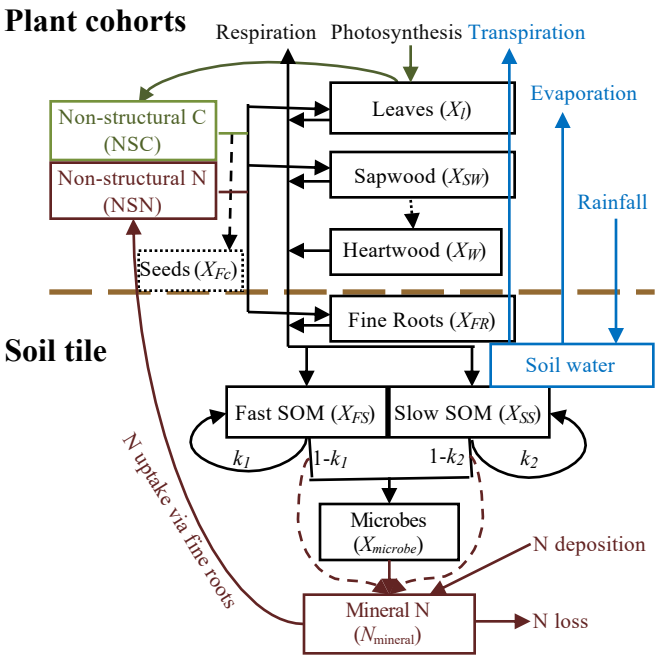

Figure E1 Biogeochemical structure of BiomeE.

The green, brown, and black lines are the flows of carbon, nitrogen, and coupled carbon and nitrogen, respectively. The green box is for carbon only. The brown boxes are nitrogen pools. The black boxes are for both carbon and nitrogen pools, where *X* can be C (carbon) and N (nitrogen). The C:N ratios of leaves, fine roots, seeds, and microbes are fixed. The C:N ratios of woody tissues, fast soil organic matter (SOM), and slow SOM are flexible. Only one tree's C and N pools are shown in this figure. The blue box and arrows are for water storage in soil and fluxes of rainfall, evaporation, and transpiration. The model can have multiple cohorts of trees, which share the same pool structure. The dashed line separates the aboveground and belowground processes.

As SOM decomposes, nitrogen in SOM is mineralized and enters into the mineral N pool when the nitrogen requirement of microbes is met. N mineralization does not simply piggyback

on the SOM decomposition because soil microbes may be limited by either C or N. The dynamics of the mineral N pool is represented by the following equation:

$$\frac{dN_{\text{mineral}}}{dt} = N_{\text{deposition}} + N_{\text{m}} - U - N_{\text{loss}}, \quad \text{(E1)}$$

where, $N_{\text{deposition}}$ is N deposition rate, assumed to be constant over the period of simulation; N_{m} is the N mineralization rate of the litter pools (fast and slow SOM and microbes); U is the N uptake rate (gN m^{-2} $hour^{-1}$) of plant roots; and N_{loss} includes the loss of mineralized N by denitrification and runoff. The N deposition ($N_{\text{deposition}}$) is the only N input to the ecosystem.

Total N mineralization rate (N_{m}) is computed from the decomposition from fast and slow SOMs and turnover of microbes. The decomposition processes of SOMs are represented by a model modified from (Manzoni et al., 2010). In this model, the out-flux of C from the i^{th} pool ($C_{i,\text{out}}$) is calculated by:

$$C_{i,\text{out}} = \xi(T, M)\rho_i QC_i \ , \quad \text{(E2)}$$

where, ξ is the response function of decomposition to soil temperature (T) and moisture (M), taken as the average of the values in the top 0.2 meters of the soil in the soil hydrology and energy model in Weng *et al*. (2105), ρ_i is the basal turnover rate of the i^{th} litter pool at reference temperature and moisture, QC_i is the C content in i^{th} pool.

Then, the out-flux of N from the i^{th} pool ($N_{i,\text{out}}$) is:

$$N_{i,\text{out}} = \xi(T, M)\rho_i QN_i \ , \quad \text{(E3)}$$

where, QN_i is the N content in the i^{th} pool.

The mineralized N ($N_{i,\text{mineralizedN}}$) at this step is the difference between the out-flux of N from the i^{th} pool and the N used to build microbes:

$$N_{i,\text{mineralizedN}} = \max\left(0, N_{i,\text{out}} - \frac{\varepsilon_0 \cdot C_{i,\text{out}}}{\Lambda_{\text{microbe}}}\right), \quad \text{(E4)}$$

where, ε_0 is default carbon-use efficiency of litter decomposition, Λ_{microbe} is microbe's C:N ratio. And, the N flux from the i^{th} litter pool to the microbial pool ($N_{i,\text{microbe}}$) is:

$$N_{i,\text{microbe}} = N_{i,\text{out}} - N_{i,\text{mineralizedN}}. \quad \text{(E5)}$$

Thus, the actual carbon use efficiency of the i^{th} litter pool (ε_i) is:

$$\varepsilon_i = \frac{C{:}N_{\text{microbe}} \cdot N_{i,\text{microbe}}}{C_{i,\text{out}}}. \quad \text{(E6)}$$

The carbon change in microbial pool ($\Delta C_{\text{microbe}}$) is then calculated as:

$$\Delta C_{\text{microbe}} = \sum_i (1 - k_i) \Lambda_{\text{microbe}} N_{i,\text{microbe}} - \xi \rho_{\text{microbe}} Q C_{\text{microbe}}, \quad \text{(E7)}$$

where, k_i is the mixing ratio of the microbes with the i^{th} litter pool, ρ_{microbe} is the basal turnover rate of the microbe pool at reference temperature and moisture, QC_{microbe} is the C content in the microbe pool. The N change in microbial pool ($\Delta N_{\text{microbe}}$) is:

$$\Delta N_{\text{microbe}} = \sum_i (1 - k_i) N_{i,\text{microbe}} - \xi \rho_{\text{microbe}} Q N_{\text{microbe}}, \quad \text{(E8)}$$

where, QN_{microbe} is the N content in the microbe pool.

The C changes in the i^{th} litter pool (ΔC_i) is:

$$\Delta C_i = LitterC_i + k_i \sum_i \Lambda_{\text{microbe}} N_{i,\text{microbe}} - \xi \rho_i C_i, \quad \text{(E9)}$$

where, $LitterC_i$ is litter C input from litterfall to the i^{th} litter pool. And, the N changes in the i^{th} litter pool (ΔN_i) is:

$$\Delta N_i = LitterN_i + k_i \sum_i N_{i,\text{microbe}} - \xi \rho_i N_i, \quad \text{(E10)}$$

where, $LitterN_i$ is litter N input from litterfall to the i^{th} litter pool. Then, the total N mineralization ($N_{\text{mineralized}}$) rate is calculated as follows:

$$N_{\text{mineralized}} = \sum_i N_{i,\text{mineralizedN}} + \xi \rho_{\text{microbe}} N_{\text{microbe}} \cdot \quad \text{(E11)}$$

413 And, the heterotrophic respiration (R_{h}) is:

$$R_{\text{h}} = \sum_i (1 - \varepsilon_i) C_{i,\text{out}} + \xi \rho_{\text{microbe}} C_{\text{microbe}} \quad \text{(E12)}$$

414

415 In our model, the N loss (N_{loss}) from the mineral N pool is calculated by:

$$N_{loss} = N \cdot [(1 - e^{-\eta W_{\text{runoff}}}) + k_{N,25} \cdot e^{\left[\frac{E_{\text{a,den}}(T-25)}{298R(T+273)}\right]} \quad \text{(E13)}$$

416 where W_{runoff} is the rate of water runoff (kg m^{-2} hour^{-1}) predicted by the soil water dynamics
417 module, η is a parameter for mineral N taken out by runoff, $k_{N,25}$ is the denitrification rate at
418 25 °C, $E_{\text{a,den}}$ is active energy of denitrification (49860 J mol^{-1}), R is gas constant (8.31 J mol^{-1} K^{-1}
419). We turned off N_{loss} in our simulations of this study by setting η and $k_{N,25}$ as zero.

420

421

422 **Table E1 Parameters**

Symbol	Definition	Unit	Default value
$f_{U,max}$	Maximum mineral N absorption rate	$hour^{-1}$	0.5
K_{FR}	Root biomass at which the N-uptake rate is half of the maximum	Kg C m^{-2}	0.3
CN_{FR}	Target C:N ratio of fine roots	Kg C kgN^{-1}	60
q_N	Multiple of target leaf and root nitrogen to target NSN	-	5.0
ε_0	Default carbon-use efficiency of litter decomposition	-	0.4
$C{:}N_{microbe}$	Microbial C:N ratio	Kg C kgN^{-1}	10
$\rho_{microbe}$	Turnover rate of the microbe pool at reference temperature and moisture	yr^{-1}	2.5
ρ_1	Turnover rate of fast SOM pool at reference temperature and moisture	yr^{-1}	1.25
ρ_2	Turnover rate of sow SOM pool at reference temperature and moisture	yr^{-1}	0.1
k_1	Mixing ratio of the microbes with fast SOM pool	-	0.8
k_2	Mixing ratio of the microbes with slow SOM pool	-	0.8
H	Parameter for N taken out by runoff	$hour^{-1}$ kg H_2O^{-1}	0.05
$k_{N,25}$	Denitrification rate at 25 °C	yr^{-1}	2.0
$E_{a,den}$	Active energy of denitrification	J mol^{-1}	49860

423

424

F. Root Water Uptake and Soil Water Dynamics

Calculations of water uptake by roots closely follow the model described in Weng et al., (2015). We define maximum water uptake rate (i.e., "water supply," U_{max}) as the amount of water an individual plant can potentially uptake from soil. Water demand (U_d, Eq. A20) is the amount of water needed for non-water-limited photosynthesis, and uptake is the amount of water the plant actually gets. If supply (U_{max}) is greater than demand (U_d), then the plant is not water-limited, and the uptake will equal the demand. If supply is less than demand, then the plant is water-limited, and uptake will be equal to supply. U_{max} is calculated following Darcy's law in the approximation of quasi-steady flow in a small vicinity of fine roots. We use this model to derive an expression for water uptake as a function of xylem water potential. Setting xylem water potential equal to the plant permanent wilting point yields the value of U_{max} needed for Eq. A21. In the following, u is the water uptake rate per unit length of fine root (kg m^{-1} s^{-1}) at a given soil depth, R is the characteristic radial half-distance between fine roots (m), r_r is the root radius (m), and r the distance from the root axis (m).

For steady flow toward the root,

$$u = 2\pi r K(\psi)\frac{d\psi}{dr} \tag{F1}$$

where $K(\psi)$ is unsaturated hydraulic conductivity (kg m^{-2} s^{-1}),

$$K(\psi) = \begin{cases} K_s\left(\frac{\psi}{\psi_*}\right)^{-(2+3/b)}, & \psi \le \psi_* \\ K_s, & \psi > \psi_* \end{cases} \tag{F2}$$

where K_S is the conductivity of saturated soil, b is an empirical coefficient, ψ is the soil water potential (m), and ψ_* is the air entry water potential. Note that since the flow is assumed to be in steady-state, u doesn't depend on r; i.e., ψ, and thus $K(\psi)$, are functions of r such that $u(r)$ (Eq.

F1) is constant (Gardner, 1960). Integrating from the root-soil interface (i.e., the root surface) to the half-distance R between fine roots (with potential ψ_s at that distance from the root axis, and ψ_r at the root surface):

$$\int_{r_r}^{R} \frac{u}{2\pi r} dr = \int_{\psi_r}^{\psi_s} K(\psi) d\psi \qquad \text{(F3)}$$

where ψ_r is water potential at the root surface, and ψ_s — at the distance R from the root. The macro-scale water movement in the soil, and, consequently, water potential ψ_s is calculated as in the LM3 model (see Milly et al., 2014 for detail). Equation (F3) can be rewritten in a more convenient form:

$$u = \frac{2\pi}{\ln(R / r_r)} \int_{\psi_r}^{\psi_s} K(\psi) d\psi \qquad \text{(F4)}$$

This relationship is assumed to hold in a soil layer at a given vertical depth in our case.

The integral on the right-hand side of Eq. F4 is called matric flux potential (Raats, 2007). The water flux through the root surface (i.e., membrane of surface cells) per unit length of root is:

$$u = 2\pi r_r K_r (\psi_r - \psi_x) \qquad \text{(F5)}$$

where K_r is permeability of root membrane per unit membrane area (kg m^{-2} area m^{-1} water potential gradient per second, kg m^{-3} s^{-1}), and ψ_x is root xylem water potential (m).

To calculate the characteristic half-distance between roots R (m), we suppose cohort i has specific root length λ_i (length of fine roots per unit mass of fine root carbon; m kg^{-1} C) and fine root biomass per individual plant per unit soil depth $b_{r,i}$ (kg C m^{-1}; where $b_{r,i}$ depends on total plant fine-root mass and soil depth according to Eq. F9). The total length of fine roots of all

cohorts per unit volume of soil (m m^{-3}) at a given soil depth is $\sum_i n_i \lambda_i b_{r,i}$ (where n_i is the density of individuals per unit ground area in cohort *i*), and its reciprocal is the mean area (m^2) of soil cross-section surrounding each root. Solving for the radius of a circle with this area yields

$$R = \left(\pi \sum_i n_i \lambda_i b_{r,i} \right)^{-1/2} . \quad \text{(F6)}$$

Combining Eqs F2, F4, and F5, we get:

$$r_r K_r (\psi_r - \psi_x) = \frac{2\pi K_s}{\ln(R/r_r)} \left\{ -\frac{\psi_*}{1+3/b_{r,i}} \left[\left(\frac{\min(\psi_s, \psi_*)}{\psi_*} \right)^v - \left(\frac{\min(\psi_r, \psi_*)}{\psi_*} \right)^v \right] \right. \quad \text{(F7)}$$
$$\left. - \max(0, \psi_r - \psi_*) + \max(0, \psi_s - \psi_*) \right\}$$

where $v \equiv -(1 + 3/b)$, and b is defined in Eq. F2. Given xylem water potential ψ_x (see following paragraph) and soil water potential ψ_s, we can get the water potential at the root-soil interface ψ_r and, consequently, the water uptake per unit root length $u = u(\psi_x, \psi_s)$ at a given soil depth from Eq. F5.

In this model, we assume no resistance to water flow in the xylem. Root xylem water potential (m) increases linearly with depth so that $\psi_x = \psi_{x0} + z$, where ψ_{x0} is the root xylem potential at the ground surface and z is depth. The total uptake by an individual plant then is the vertical integral over soil depth (discretized as a sum across soil layers *j*, properly weighted):

$$U(\psi_{x0}) = \sum_{j=1}^{N} u(\psi_{x0} + z_j, \psi_{s,j}) L_j S_j \quad \text{(F8)}$$

where z_j is the depth midpoint of layer *j*, $\psi_{s,j}$ is the soil water potential in the layer, and L_j is the total length of the individual plant's roots in soil layer *j*. The factor S_j turns off uptake ($S_j = 0$) when certain conditions are met, e.g., if there is ice in the layer or the uptake is negative. The

maximum plant water uptake rate ("supply") U_{max} is calculated from Eq. F8 with the xylem water potential at the ground surface (ψ_{x0}) set equal to the permanent wilting point ψ_{wilt}: $U_{max} = U(\psi_{wilt})$. Again, if this supply (U_{max}) is smaller than non-water-limited demand (U_d; Eq. A20), then photosynthesis and stomatal conductance are modified according to the reduction factor (Eq. A21). Alternatively, if $U_{max} \geq U_d$, then ψ_{x0} is determined by setting whole-plant uptake equal to U_d.

The vertical distribution of fine roots determines root biomass in each soil layer and therefore the length of roots in a soil layer. It is assumed to be distributed exponentially in soil (Jackson et al., 1997):

$$b(z) = \frac{B_r}{\zeta} \exp\left(-\frac{z}{\zeta}\right) \quad \text{(F9)}$$

where $b(z)$ is fine root biomass per unit depth (kg C m^{-1}) as a function of soil depth z (m), B_r is the individual plant's total biomass of fine roots, and ζ is a species-specific (or PFT-specific) *e*-folding depth of vertical distribution of fine roots. ζ is set as 0.29 m for the temperate deciduous trees in this study. The vertical integral of $b(z)$ is equal to the total biomass of fine roots, B_r. The biomass of fine roots in each soil layer is calculated as a vertical integral of Eq. F9 over the depth of the layer. The total soil depth in this study is set to 2 m, subdivided in 3 layers with thickness of 0.05, 0.45, and 1.5 m, respectively.

Soil water dynamics is simulated following a soil water bucket model as described in Weng and Luo (2008), which includes the processes of soil water refilling by precipitation, soil surface evaporation, and runoff. Soil water content in each layer is updated hourly according to the budget of precipitation, transpiration, surface evaporation, and runoff.

$$\frac{dW_i(t)}{dt} = Precip_i(t) - Transp_i(t) - Evap_i(t) - Runoff_i(t) \quad \text{(F10)}$$

where, W_i is soil water content in layer i (kg m^{-2}), $Precip_i$ is the water supply at layer i from precipitation (kg m^{-2} s^{-1}), Transp is water absorbed by plant root in layer i (kg m^{-2} s^{-1}), $Evap_i$ is the water evaporated in layer i (kg m^{-2} s^{-1}) (it happens only in the first layer). Water from precipitation flows to each soil layer sequentially when the upper layer is filled. The layers that a rainfall event can fill depends on precipitation amount, soil water holding capacity, and current soil water content. The excessive water after all the three layer are filled to their water holding capacity becomes runoff.

Soil surface evaporation only happens in the first layer of soil. It is calculated with the Penman-Monteith equation (Monteith, 1965):

$$Evap = \frac{\Delta R_n^* + \rho_a c_p D_{air}/r_{aero}}{\Delta + \gamma(1+\frac{r_{soil}}{r_{aero}})}/\lambda \quad \text{(F11)}$$

where, Δ is the rate of change of saturation specific humidity with air temperature (Pa K^{-1}), R_n^* is net radiation received at soil surface (W m^{-2}), c_p is specific heat capacity of air (J kg^{-1} K^{-1}) ρ_a is dry air density (kg m^{-3}), D_{air} is vapor pressure deficit (Pa), r_{aero} is atmospheric resistance (s m^{-1}), r_{soil} is soil resistance (s m^{-1}), γ is psychrometric constant ($\approx$ 66 Pa K^{-1}), λ is latent heat of vaporization (J g^{-1}).

G. Plant Phenology

The phenology for cold-deciduous plants used in the examples presented in this paper is described. The onset of a growing season is controlled by two variables, growing degree days (GDD), and a weighted mean daily temperature (T_{pheno}). The two variables are computed by the following equations:

$$GDD(t) = \sum_{i=1}^{t} \max\left[T_d(t) - 5℃, 0\right] \quad \text{(G1)}$$

$$T_{pheno}(t) = \begin{cases} T_d(t) & when\ t = 1 \\ 0.8T_{pheno}(t-1) + 0.2T_d(t) & when\ t > 1 \end{cases} \quad \text{(G2)}$$

where t is the number of days from the end date of the last growing season and $T_d(t)$ is the daily mean temperature at day t. There are two thresholds for these two variables, GDD_{crit} (320 day·°C) and T_{crit} (10 °C), respectively. When the criteria $GDD(t) > GDD_{crit}$ and $T_{pheno}(t) > T_{crit}$ are met, a growing season is initiated by setting $p(t) = 1$. The ending of a growing season is controlled by T_{pheno}. When $T_{pheno}(t)$ falls below T_{crit}, the growing season is turned off ($p(t)$=0), leaves begin to senesce at an assumed rate (γ_L). A fraction of carbon (0.25) of senesced leaves is retranslocated to the NSC pool at leaf falling.

References:

Bohlman, S. and Pacala, S.: A forest structure model that determines crown layers and partitions growth and mortality rates for landscape-scale applications of tropical forests: Canopy layer model, Journal of Ecology, 100(2), 508–518, doi:10.1111/j.1365-2745.2011.01935.x, 2012.

Collatz, G., Ribas-Carbo, M. and Berry, J.: Coupled Photosynthesis-Stomatal Conductance Model for Leaves of C4 Plants, Functional Plant Biol., 19(5), 519, doi:10.1071/PP9920519, 1992.

Collatz, G. J., Ball, J. T., Grivet, C. and Berry, J. A.: Physiological and environmental regulation of stomatal conductance, photosynthesis and transpiration: a model that includes a laminar boundary layer, Agricultural and Forest Meteorology, 54(2–4), 107–136, doi:10.1016/0168-1923(91)90002-8, 1991.

Farquhar, G. D., Caemmerer, S. V. and Berry, J. A.: A biochemical model of photosynthetic CO2 assimilation in leaves of C3 species, Planta, 149(1), 78–90, doi:10.1007/BF00386231, 1980.

Farrior, C. E., Dybzinski, R., Levin, S. A. and Pacala, S. W.: Competition for Water and Light in Closed-Canopy Forests: A Tractable Model of Carbon Allocation with Implications for Carbon Sinks, American Naturalist, 181(3), 314–330, doi:10.1086/669153, 2013.

Gardner, W. R.: Dynamic aspects of water availability to plants, Soil Science, 89(2), 63–73, doi:10.1097/00010694-196002000-00001, 1960.

Gerber, S., Hedin, L. O., Oppenheimer, M., Pacala, S. W. and Shevliakova, E.: Nitrogen cycling and feedbacks in a global dynamic land model, GLOBAL BIOGEOCHEMICAL CYCLES, 24, doi:10.1029/2008GB003336, 2010.

Jackson, R. B., Mooney, H. A. and Schulze, E.-D.: A global budget for fine root biomass, surface area, and nutrient contents, Proceedings of the National Academy of Sciences, 94(14), 7362–7366, doi:10.1073/pnas.94.14.7362, 1997.

Leuning, R., Kelliher, F. M., Pury, D. G. G. and Schulze, E.-D.: Leaf nitrogen, photosynthesis, conductance and transpiration: scaling from leaves to canopies, Plant Cell Environ, 18(10), 1183–1200, doi:10.1111/j.1365-3040.1995.tb00628.x, 1995.

Manzoni, S., Trofymow, J. A., Jackson, R. B. and Porporato, A.: Stoichiometric controls on carbon, nitrogen, and phosphorus dynamics in decomposing litter, Ecological Monographs, 80(1), 89–106, 2010.

McMurtrie, R. E., Iversen, C. M., Dewar, R. C., Medlyn, B. E., Näsholm, T., Pepper, D. A. and Norby, R. J.: Plant root distributions and nitrogen uptake predicted by a hypothesis of optimal root foraging, Ecology and Evolution, 2(6), 1235–1250, doi:10.1002/ece3.266, 2012.

Medvigy, D., Wofsy, S. C., Munger, J. W., Hollinger, D. Y. and Moorcroft, P. R.: Mechanistic scaling of ecosystem function and dynamics in space and time: Ecosystem Demography model

563 version 2, JOURNAL OF GEOPHYSICAL RESEARCH-BIOGEOSCIENCES, 114,
564 doi:10.1029/2008JG000812, 2009.

565 Milly, P. C. D., Malyshev, S. L., Shevliakova, E., Dunne, K. A., Findell, K. L., Gleeson, T.,
566 Liang, Z., Phillipps, P., Stouffer, R. J. and Swenson, S.: An Enhanced Model of Land Water and
567 Energy for Global Hydrologic and Earth-System Studies, Journal of Hydrometeorology, 15(5),
568 1739–1761, doi:10.1175/JHM-D-13-0162.1, 2014.

569 Monteith, J. L.: Evaporation and environment, Symp. Soc. Exp. Biol., 19, 205–234, 1965.

570 Moorcroft, P. R., Hurtt, G. C. and Pacala, S. W.: A method for scaling vegetation dynamics: The
571 ecosystem demography model (ED), Ecological Monographs, 71(4), 557–585,
572 doi:10.1890/0012-9615(2001)071[0557:AMFSVD]2.0.CO;2, 2001.

573 Polgar, C. A. and Primack, R. B.: Leaf-out phenology of temperate woody plants: from trees to
574 ecosystems: Tansley review, New Phytologist, 191(4), 926–941, doi:10.1111/j.1469-
575 8137.2011.03803.x, 2011.

576 Purves, D. W., Lichstein, J. W., Strigul, N. and Pacala, S. W.: Predicting and understanding
577 forest dynamics using a simple tractable model, PROCEEDINGS OF THE NATIONAL
578 ACADEMY OF SCIENCES OF THE UNITED STATES OF AMERICA, 105(44), 17018–
579 17022, doi:10.1073/pnas.0807754105, 2008.

580 Shevliakova, E., Pacala, S. W., Malyshev, S., Hurtt, G. C., Milly, P. C. D., Caspersen, J. P.,
581 Sentman, L. T., Fisk, J. P., Wirth, C. and Crevoisier, C.: Carbon cycling under 300 years of land
582 use change: Importance of the secondary vegetation sink, Global Biogeochemical Cycles, 23,
583 GB2022, doi:10.1029/2007GB003176, 2009.

584 Shinozaki, Kichiro, Yoda, Kyoji, Hozumi, Kazuo and Kira, Tatuo: A quantitative analysis of
585 plant form – the pipe model theory. I. Basic analyses, Japanese Journal of Ecology, 14(3), 97–
586 105, 1964.

587 Strigul, N., Pristinski, D., Purves, D., Dushoff, J. and Pacala, S.: Scaling from trees to forests:
588 tractable macroscopic equations for forest dynamics, Ecological Monographs, 78(4), 523–545,
589 doi:10.1890/08-0082.1, 2008.

590 Weng, E. and Luo, Y.: Soil hydrological properties regulate grassland ecosystem responses to
591 multifactor global change: A modeling analysis, J. Geophys. Res., 113(G3), G03003,
592 doi:10.1029/2007JG000539, 2008.

593 Weng, E., Farrior, C. E., Dybzinski, R. and Pacala, S. W.: Predicting vegetation type through
594 physiological and environmental interactions with leaf traits: evergreen and deciduous forests in
595 an earth system modeling framework, Global Change Biology, 23(6), 2482–2498,
596 doi:10.1111/gcb.13542, 2017.

597 Weng, E. S., Malyshev, S., Lichstein, J. W., Farrior, C. E., Dybzinski, R., Zhang, T.,
598 Shevliakova, E. and Pacala, S. W.: Scaling from individual trees to forests in an Earth system

599 modeling framework using a mathematically tractable model of height-structured competition,
600 Biogeosciences, 12(9), 2655–2694, doi:10.5194/bg-12-2655-2015, 2015.

601 Wesołowski, T. and Rowiński, P.: Timing of bud burst and tree-leaf development in a
602 multispecies temperate forest, Forest Ecology and Management, 237(1–3), 387–393,
603 doi:10.1016/j.foreco.2006.09.061, 2006.

604 Zhang, T., Lichstein, J. W. and Birdsey, R. A.: Spatial and temporal heterogeneity in the
605 dynamics of eastern US forests: Implications for developing broad-scale forest dynamics models,
606 Ecological Modelling, 279, 89–99, doi:10.1016/j.ecolmodel.2014.02.011, 2014.

607